Cell Reports

Report

Hierarchical Size Scaling during Multicellular Growth and Development

Graphical Abstract

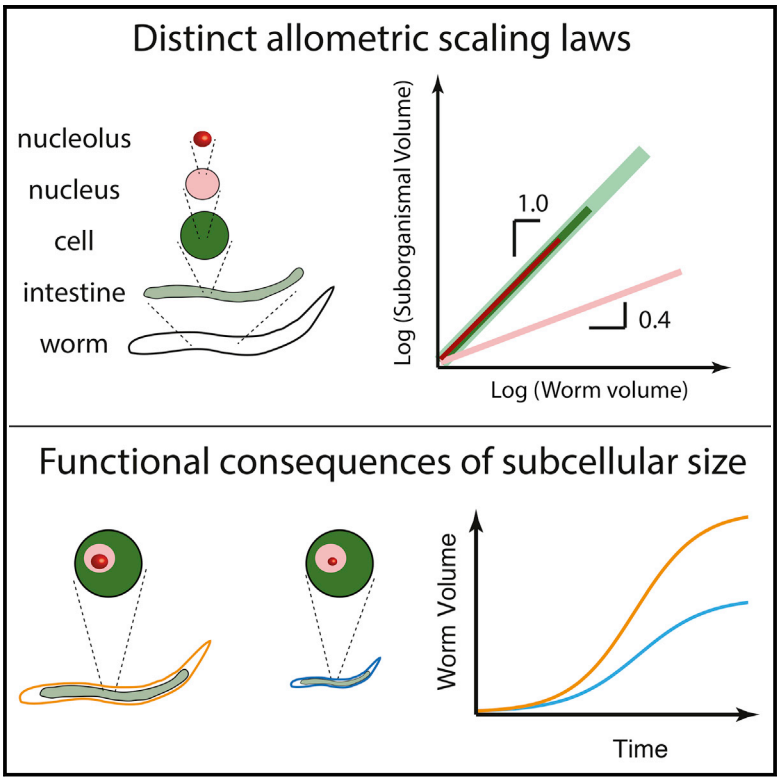

Highlights

- During multicellular growth, the nucleus does not grow as fast as the cell
- The nucleolus grows at the same rate as the cell, occupying a constant volume fraction
- Changing the volume fraction of the nucleolus results in changes in worm growth
- Larger nucleoli result in more ribosomes and could be responsible for faster growth

Authors

Sravanti Uppaluri, Stephanie C. Weber, Clifford P. Brangwynne

Correspondence

cbrangwy@princeton.edu

In Brief

Using the *C. elegans* intestinal system, Uppaluri et. al. identify distinct size-scaling laws spanning five hierarchical levels of biological organization during larval growth. This quantification establishes a connection between the size of a subcellular organelle, the nucleolus, and the whole organism by linking the organelle to worm-growth rate. Their results highlight the importance of organelle size control for organismal function.

Uppaluri et al., 2016, Cell Reports *17*, 345–352
October 4, 2016
http://dx.doi.org/10.1016/j.celrep.2016.09.007

CellPress

Cell Reports
Report

Hierarchical Size Scaling during Multicellular Growth and Development

Sravanti Uppaluri,[1,2] Stephanie C. Weber,[1,3] and Clifford P. Brangwynne[1,4,*]
[1]Department of Chemical and Biological Engineering, Princeton University, Princeton, NJ 08544, USA
[2]Present address: School of Liberal Studies, Azim Premji University, Bangalore 560100, India
[3]Present address: Department of Biology, McGill University, Montreal, QC H3A 1B1, Canada
[4]Lead Contact
*Correspondence: cbrangwy@princeton.edu
http://dx.doi.org/10.1016/j.celrep.2016.09.007

SUMMARY

Multicellular organisms must regulate their growth across the diverse length scales of biological organization, but how this growth is controlled from organelle to body, while coordinating interdependent functions at each scale, remains poorly understood. We utilized the *C. elegans* worm intestine as a model system to identify distinct allometric scaling laws, revealing that the growth of individual structures is differentially regulated during development. We show that the volume of the nucleolus, a subcellular organelle, is directly proportional (isometric) to cell size during larval development. In contrast to findings in a variety of other systems, the size of the nucleus grows more slowly and is hypoallometric to the cell. We further demonstrate that the relative size of the nucleolus, the site of ribosome biogenesis, is predictive of the growth rate of the entire worm. These results highlight the importance of subcellular size for organism-level function in multicellular organisms.

INTRODUCTION

Organisms span a fascinatingly broad range of length scales, from the sub-micron bacterium *Mycoplasma* to the 30-m blue whale. These organisms must coordinate the growth and size of their internal structures to cope with the physical and functional demands of their overall size.

Quantitative comparison of the relative growth between different biological structures, termed allometry, gives rise to power-law scaling relationships in a wide variety of systems (Huxley and Teissier, 1936). For example, an early study showed that brain size scales with body size across species spanning a wide range of sizes, from mouse to whale (Lapicque, 1907). In addition to these interspecific allometric relationships, scaling laws have also been found within a single species as it changes size during growth and development. Huxley first described such ontogenetic allometry by noting that the claw of the fiddler crab grows more quickly than its body (Huxley, 1924).

The relative sizes of subcellular structures also scale with one another. A classic example of such size scaling is the karyoplasmic ratio, which describes the proportionality between nuclear size and cell size across many different organisms and developmental stages (Hertwig, 1903; Wilson, 1896; Jorgensen et al., 2007; Neumann and Nurse, 2007). More recent studies have shown that the size of mitochondria (Rafelski et al., 2012), as well as several membrane-less organelles, including the mitotic spindle (Wühr et al., 2008; Hazel et al., 2013; Good et al., 2013), the centrosome (Decker et al., 2011), and the nucleolus (Weber and Brangwynne, 2015), all scale with the size of the cell in which they are contained. However, since these observations were made using unicellular or embryonic systems, it is not yet clear whether such subcellular scaling also occurs in a growing multicellular organism.

Increasing evidence suggests that membrane-less organelles assemble via phase separation (Brangwynne et al., 2009, 2011; Molliex et al., 2015; Weber and Brangwynne, 2015; Berry et al., 2015; Feric and Brangwynne, 2013). This mechanism intrinsically links organelle size to cell size (Berry et al., 2015; Weber and Brangwynne, 2015; Brangwynne, 2013), such that larger cells have larger organelles, given a fixed concentration of components. We recently demonstrated this in *C. elegans* embryos, where the size of the nucleolus is governed by its equilibrium with the nucleoplasmic pool of soluble components (Weber and Brangwynne, 2015). Size scaling of the nucleolus is particularly interesting because of its function in ribosome biogenesis, which couples the nucleolus to cell and organism growth. Indeed, in the worm *C. elegans*, mutations that affect the size and activity of the nucleolus result in increased cell and body size (Frank and Roth, 1998).

Despite a century of size-scaling observations, the mechanisms coordinating the growth and size of structures at different length scales, particularly in multicellular organisms, remain largely elusive. Even less is understood about the functional consequences of size scaling. Nevertheless, these are of particular interest since dysregulation in size control is a hallmark of many diseases (Edens et al., 2013; Yang and Xu, 2011; Derenzini et al., 2009).

Here, we use *C. elegans* as a model to investigate how growth and size are coordinated across several levels of biological organization from tissues, to cells, to organelles. We found that the sizes of two different organelles—the nucleolus and the nucleus, as well as the cell and the intestine—all scale with one another in a developing multicellular organism. We show that nucleolar size scales linearly with cell size. In contrast, nuclear

size does not keep up with cell size, resulting in a decreasing karyoplasmic ratio through larval growth and development. Using genetic perturbations, we show that an increased ratio of nucleolar size to cell size correlates with faster worm growth rates. These results suggest that size control across hierarchical biological structures has important functional consequences for organismal growth.

RESULTS

Following embryogenesis, a *C. elegans* larva emerges from its eggshell at ~250 μm in length. As larval development proceeds (from larval stage L1 to L4), the worm grows over 100-fold in volume before reaching adulthood. We investigated how this growth is coordinated at the tissue, cell, and organelle levels.

Most of the worm's increase in size arises from hypertrophic cell growth rather than from cell division. For example, the worm intestine is composed of 20 cells that do not divide during postembryonic development. Nevertheless, this tissue spans nearly the entire length of the body as the worm grows and develops. The intestinal tissue, therefore, provides a useful model system to study size scaling from the subcellular level to the organismal level during growth and development. To quantify cell and tissue growth, we visualized intestinal cells using a transgenic line that expresses the pleckstrin homology domain (PH) fused to GFP under an intestine-specific promoter (Figure 1). This transgene localizes to cell membranes, revealing the nine-ring structure of the intestine. The first ring, "int1," is made up of four cells, while the remaining eight (int2–int9) comprise two cells each (McGhee, 2007), as illustrated in Figure 1A. The int1 cells are roughly half the size of int2 cells (all of which remain mononucleate through development) and remain so despite an ~100-fold volume increase through development.

To determine whether the size of subcellular structures also differed between these cell types, we constructed a line expressing FIB-1 (a conserved nucleolar protein) fused to mCherry, under the same intestinal promoter (Figure 1A). We note that, although this is just one protein in a multi-component structured organelle, we used the extent of concentrated FIB-1 localization as a proxy for nucleolar size; a number of other conserved nucleolar components, such as DAO-5, colocalize with FIB-1 (Weber and Brangwynne, 2015). While most FIB-1 assembles into the nucleolus, a soluble nucleoplasmic pool remains, allowing for simultaneous visualization of nuclei (Weber and Brangwynne, 2015).

Growth of Internal Structures during Multicellular Development

Using this worm system, we visualized the hierarchy of biological organization, as illustrated in Figure 1A. We quantified the growth of the intestine—int1 and int2 cells and their respective nuclei and nucleoli—during worm growth and development (Figures 1B–1F). We found that, at all levels of biological organization, structures do not maintain a static size but rather exhibit significant growth. Indeed, the volume of the entire intestine and its individual cells increase (Figures 1C and 1D) in proportion to the whole organism (Figure S1).

Throughout development, the volume of int2 cells is roughly twice the volume of int1 cells (Figure 1D). As with cell volume (V_c), nucleolar volume (V_{no}) of int2 cells is always larger than that of int1 cells and also increases ~100-fold through development (Figure 1F). In contrast to cell and nucleolar size, however, nuclear size (V_n) is about the same for both int1 and int2 cell types until ~60 hr, by which time the worm has reached adulthood (Figure 1E). Thus, while all internal structures increase in size during multicellular development, their growth appears to be differentially regulated.

Hierarchical Size Scaling during Larval Development

Next, we examined how the worm coordinates the growth of these internal structures with respect to one another. Using quantitative imaging, we observed that, throughout larval development, nucleolar size scales linearly with cell size (Figures 2A and 2C). Ribosomal output is correlated to nucleolar size (Frank and Roth, 1998; Frank et al., 2002), and drives cell growth (Montagne et al., 1999; Scott et al., 2010). Thus, the nucleolar size scaling that we observed likely reflects the functional need for ribosomes during growth. Indeed, at about the same time that it reaches adulthood and the worm's growth slows, nucleolar size appears to plateau and stops increasing. Interestingly, however, despite significant differences in size between cell types over developmental time, this scaling remains the same for both int1 and int2 cells.

Though the nucleolus resides within the nucleus, we found, unexpectedly, that the size of the nucleus does not keep up with the size of the cell (Figure 2B), resulting in a decreasing karyoplasmic ratio throughout development (Figure 2B, inset). We further confirmed this result using a histone marker for nuclear size (see Figure S2). This finding is contrary to numerous studies in other systems, describing a roughly constant karyoplasmic ratio through development (Hertwig, 1903; Wilson, 1896; Jorgensen et al., 2007; Neumann and Nurse, 2007).

The distinction between the scaling behaviors of these organelles can clearly be seen in the log-log plot in Figure 2C. During larval development, the volume of the nucleolus scales roughly linearly with the volume of the cell: $V_{no} \sim V_c^{\alpha}$, with α = 0.9 ± 0.06. This nearly isometric scaling $(\alpha = 1)$ is also seen in *C. elegans* embryos (Weber and Brangwynne, 2015) but may be particularly important in these growing larvae, due to the ribosomal requirements of growth. On a log-log plot, it is clear that the volume of the nucleus, by contrast, scales sublinearly with cell volume: $V_n \sim V_c^{\beta}$, with β = 0.4 ± 0.04. This hypoallometric scaling $(\beta < 1)$ in larval worms is different from our observations in embryos (see Figure S2), raising the question of whether nuclear size is regulated to cope with the challenges of exponential growth.

We showed previously that nucleolar size is dependent on the degree to which the concentration (C_n) of nucleolar protein components exceeds a threshold concentration (Weber and Brangwynne, 2015), as predicted by a liquid phase transition model. Indeed, consistent with this and other reports that nucleoli behave as liquid phase droplets (Brangwynne et al., 2011; Feric and Brangwynne, 2013), fluorescence recovery after photobleaching (FRAP) experiments in adult *C. elegans* nucleoli also suggest that they have liquid-like properties (see Figure S3).

Interestingly, here, we found that the total cellular concentration C_c of FIB-1 decreases throughout post-embryonic

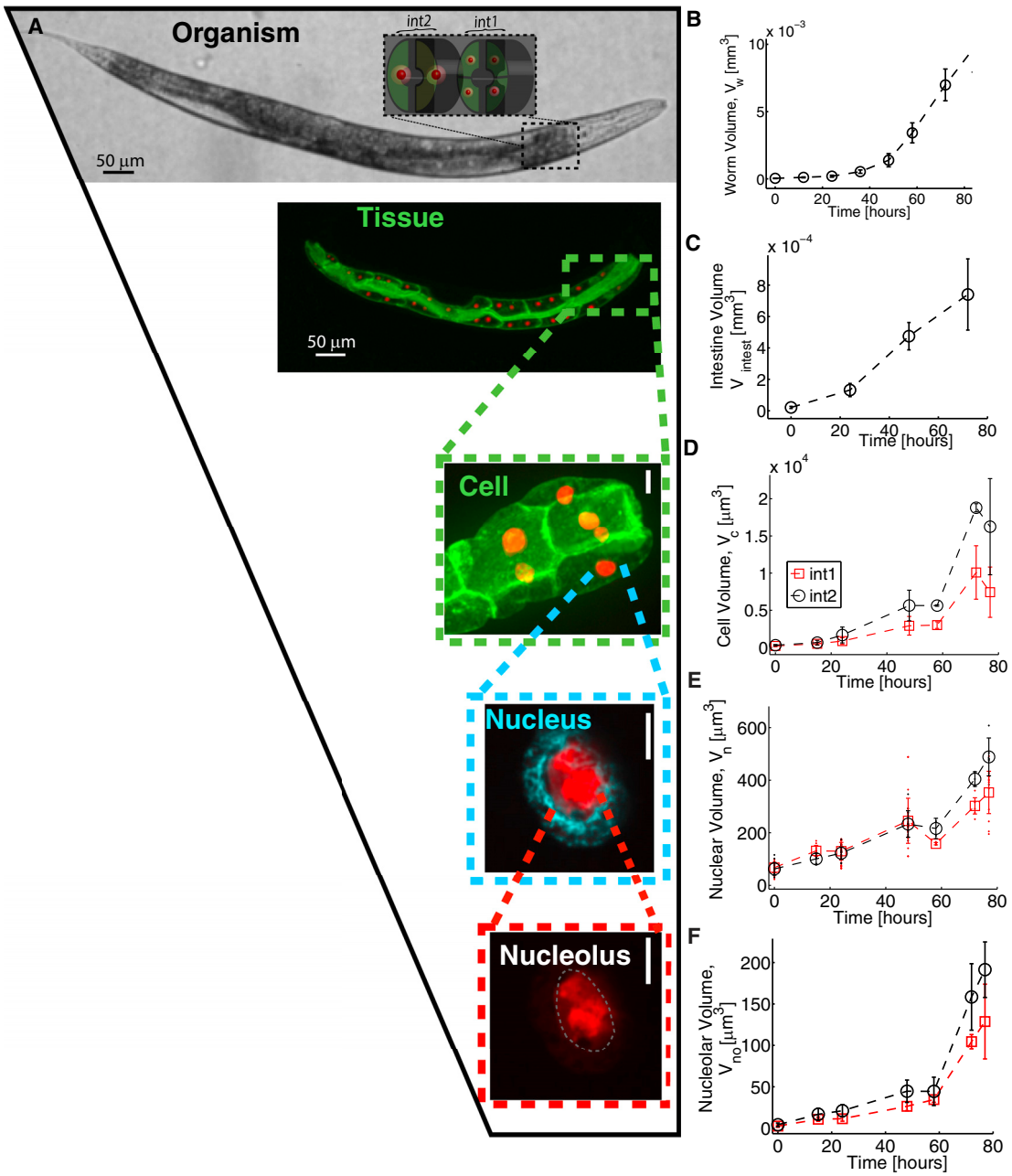

Figure 1. All Levels of Biological Organization Grow during Development

(A) Hierarchical organization; organism to tissue to cell to nucleus to organelle. Scale bar 10 μm unless specified. Inset of top panel: schematic of int1 and int2 rings.

(B) Organism volume growth over time; n = 10.

(C) Intestinal volume growth in time; n = 10.

(D) Cell volume growth over time. Legend is the same for (D)–(F).

(E) Nuclear volume growth over time. Nucleus, histone marker is indicated in cyan; n = 71.

(F) Nucleolar volume increase in size over time; n = 71.

Black indicates int2 cells, and red indicates int1 cells. Data are shown as mean ± SD.

development (see Figure S3). In this regime of decreasing C_c,if the karyoplasmic ratio were conserved during larval development, as it is during early embryogenesis, nucleoplasmic concentration would also decrease. However, the decrease in karyoplasmic ratio that we measure (Figure 2B, inset) may serve to limit this effect by concentrating nucleolar components within

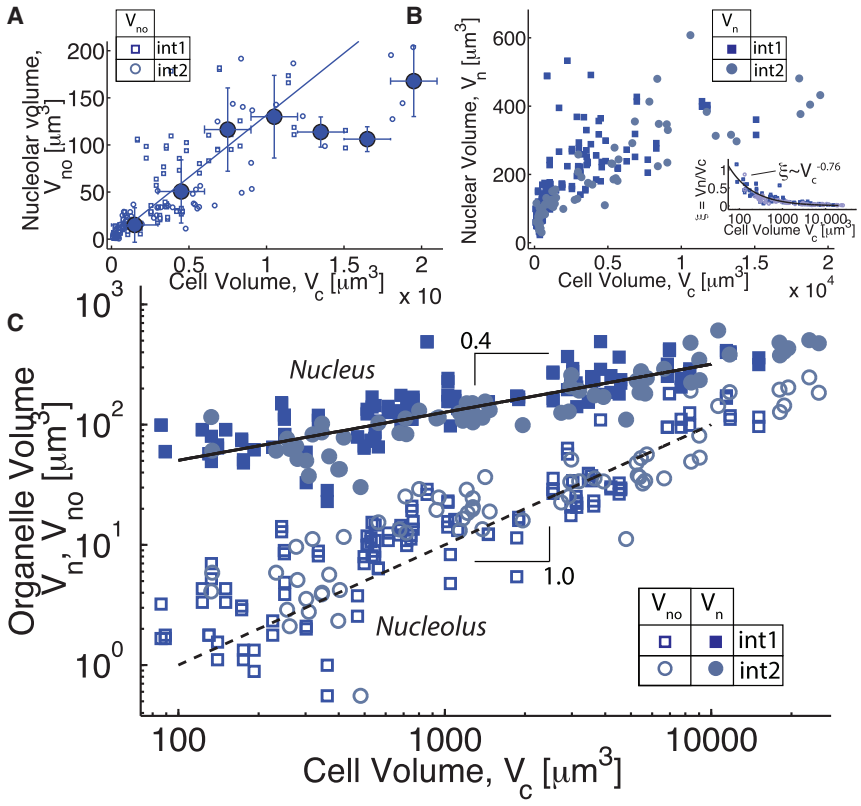

Figure 2. Allometry of Subcellular Structures with Cell Volume

Squares and circles indicate int1 and int2 structures, respectively. Open symbols are nucleoli, and solid symbols are nuclei.

(A) Nucleolar volume, V_{no}, as a function of cell size, V_c. V_{no} scales linearly with cell size during larval development in both int1 and int2 cells. Raw data (smaller symbols) and mean ± SD across bins are shown with linear fit ($R^2_{WT} = 0.91$), n = 71.

(B) Nuclear volume, V_n, as a function of cell size, V_c. Inset: karyoplasmic ratio $\xi = V_n/V_c$ decreases as the cell grows, with $\xi \sim V_c^{\kappa}$, $\kappa = -0.76 \pm 0.06$.

(C) Nucleoli are isometric with cell size, while nuclei are hypoallometric, as shown by linear fit on the log-log plot. As discussed later, these relations hold in the mutants of different size.

See also Table S1.

the smaller nucleus. We speculate that such a decreasing karyoplasmic ratio could allow for the assembly of larger nucleoli in larger cells without having to increase nucleolar protein production exponentially as the organism grows (see Supplemental Information).

Genetic Perturbations Change Nucleolar Size-Scaling Relationships

Next, we sought to test the robustness of these organelle and cellular scaling relationships by examining mutant worms of various body sizes (Figure 3A). We crossed our fluorescent transgenic line into the *sma-1* and *ncl-1* genetic backgrounds. SMA-1 determines the rate of elongation during embryogenesis (McKeown et al., 1998), and these mutants are smaller than wild-type (WT) worms from the L1 stage through adulthood. NCL-1 is a negative regulator of rRNA synthesis and cell growth, and *ncl-1* mutants exhibit enlarged nucleoli, cells, and worm bodies (Frank and Roth, 1998). We found that int1 cells in the *sma-1* worms are consistently smaller than those in the WT worms, while those in *ncl-1* worms are consistently larger, as seen in Figure 3B. This trend is also seen for int2 cells (see Figure S4).

The scaling between nucleolar size and cell size for both mutant backgrounds exhibits a similar form as that in WT (Figure 3C): a linear increase in nucleolar size with cell size during larval growth ($V_{no} \sim V_c^{\alpha}$, with $\alpha \sim 1$), followed by a plateau regime on reaching adulthood. Importantly, the hypoallometric scaling between nuclear and cell size is also seen in the mutants with $V_n \sim V_c^{\beta}$, where $\beta < 1$ (see Table S1 for a complete list of scaling exponents). The scaling data from these mutants further support the idea that a decreasing karyoplasmic ratio could serve to concentrate nuclear proteins for the assembly of larger nucleoli (Table S1).

We note, however, that the quantitative relationship between nucleolar size and cell size varies significantly. The linear fits shown in Figure 3C yield the volume fraction of the cell occupied by the nucleolus ($\phi = V_{no}/V_c$) during larval development. Figure 3D illustrates that $\phi_{sma} < \phi_{WT} < \phi_{ncl}$.

Functional Consequence of Scaling: Increased Volume Fraction Correlates with Faster Growth

We hypothesized that the scaling relationships between nucleolar size and cell size observed in Figure 3C would have an impact on organismal growth. We quantified worm growth through larval development in the three genetic backgrounds, as shown in Figure 4A. The growth curves for each genetic background exhibit a logistic form, where the worm volume can be fit to $V_W = V^{max}/1 + e^{-k\,(t-t_0)}$, with k representing a maximal growth rate and V^{max} representing the maximum worm volume. Consistent with an impact of nucleolar size on worm growth, k correlates strongly with the volume fraction occupied by the nucleolus in the cell, ϕ (Figure 4B).

We sought to determine whether the trend observed in Figure 4B could serve to predict the growth rate in another genetic background. To test this hypothesis, we crossed the *ncl-1* and *sma-1* mutants and quantified the scaling relationship between nucleolar size and cell size. As seen in Figure 4D, the volume fraction occupied by nucleoli in these worms is intermediate, with $\phi_{sma} < \phi_{sma1:ncl} < \phi_{ncl}$ (Figure 4D; Figure S4); this value for ϕ is now similar to that seen in WT worms.

Interestingly, the volumetric growth rate of this mutant worm (Figure 4A) falls directly within the trend shown in Figure 4B (solid symbol), suggesting that nucleolar size scaling is predictive of the growth of the whole organism.

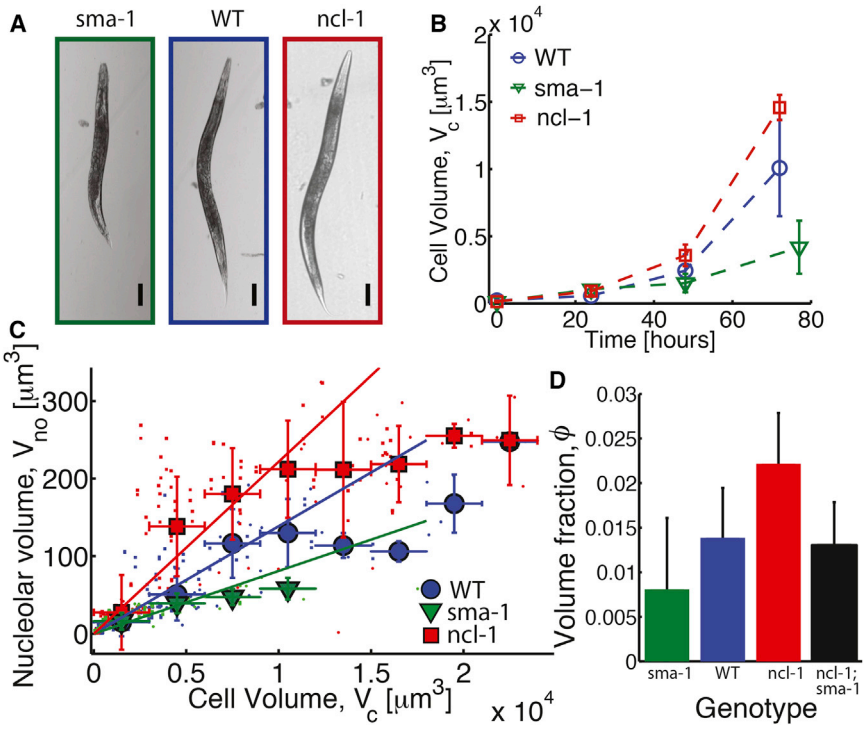

Figure 3. Organelle Size Scaling in Different Genetic Backgrounds

(A) Adult worm of each genetic background. Scale bars, 100 μm.

(B) int1 ring cell volume through development. *ncl-1* cells (n = 45) are consistently larger than WT cells (n = 71), which are consistently larger than *sma-1* cells (n = 44). Data are shown as mean ± SD.

(C) Nucleolar volume, V_{no}, scales with cell size, V_c, during larval development in all genetic backgrounds and then plateaus in adulthood. Raw data shown for both int1 and int2 cells (smaller symbols) and mean ± SD across bins are shown with fit to initial linear portion of binned data. R^2 values for goodness of linear fit are as follows: $R^2_{WT} = 0.91$, n = 71; $R^2_{ncl} = 0.91$, n = 45; and $R^2_{sma} = 0.78$, n = 44.

(D) Slopes of linear fits shown in (C) representing volume fraction of cell occupied by nucleolus. Error bars indicate 95% confidence intervals to fits.

Our findings demonstrate that, when the nucleolus occupies a larger relative volume of the cell, worms grow faster. To test whether this could be a consequence of increased ribosome production in larger nucleoli, we extracted and quantified rRNA from each of these different worm lines. rRNA extraction from identical numbers of L4 worms of each genotype shows that the total ribosomal content is smallest in sma-1 worms and largest in ncl-1 worms, with intermediate values for WT and ncl-1;sma-1 double mutant worms (Figure 4C).

These data could be used to determine the apparent ribosomal concentration per worm by normalizing by average L4 worm volume. Ribosome concentration is roughly similar to the volume fraction occupied by the nucleolus, with ncl-1 worms having the highest concentration (Figure 4D, inset). This suggests that larger nucleoli are associated with an increased level of ribosome production, as previously reported (Frank and Roth, 1998; Frank et al., 2002; Tsang et al., 2003; Rudra and Warner, 2004). Higher ribosomal concentrations imply increased protein translation capacity and, thus, likely confer faster worm growth rates, consistent with the high growth rate of the ncl-1 mutant (Figure 4D).

DISCUSSION

This work underscores the importance of multi-scale size control for coordinating function in a multicellular organism. In particular, we identify allometric scaling relationships between the nucleus, the nucleolus, and the cell that suggest a mechanism for size control of the nucleolus and further establish functional consequences in organismal growth.

Our data are consistent with nucleolar assembly being driven by liquid-liquid phase separation. Using the well-conserved nucleolar protein FIB-1, we observed that the size of the nucleolus is isometric with cell size during larval development. If the nucleus also grew isometrically, the phase separation model would require the concentration of nucleolar components within the nucleus to be maintained as constant during exponential growth, requiring a corresponding exponential increase in nucleolar components. Our finding that the nucleus, instead, scales hypoallometrically with cell size could alleviate this demand by helping to concentrate nuclear components and drive assembly of an isometrically growing nucleolus, even during large increases in cell size.

Our study focused on intestinal cells, since they do not divide; therefore, it provides a convenient platform to quantitatively study size scaling during multicellular development. Since the intestine spans nearly the entire length of the worm during larval growth, growth of the intestine mirrors that of the entire organism. However, it is possible that size scaling between organelles would depend on specific functional requirements; therefore, we have been careful to limit our observations to larval development. Indeed, once worms reach adulthood, organismal growth slows and eventually ceases (Figure 4A). This maximal worm size is coincident with a plateau in nucleolar size (Figures 2A and 3C) and may reflect a shift in the requirement for ribosomes from the intestine to other tissues, including the gonad, when metabolic needs are predominantly directed to reproduction rather than growth. Interestingly, *C. elegans* intestinal cells undergo endoreduplication during larval development, increasing in ploidy from 2n in L1 to 32n in the adult. Polyploidy has been associated with large changes in nucleolar number and body size (Lozano et al., 2006; Fankhauser and Humphrey, 1943; Fankhauser, 1939). Understanding the transition from the linear scaling regime to the plateau, as well as the effect of polyploidy on scaling, requires further investigation

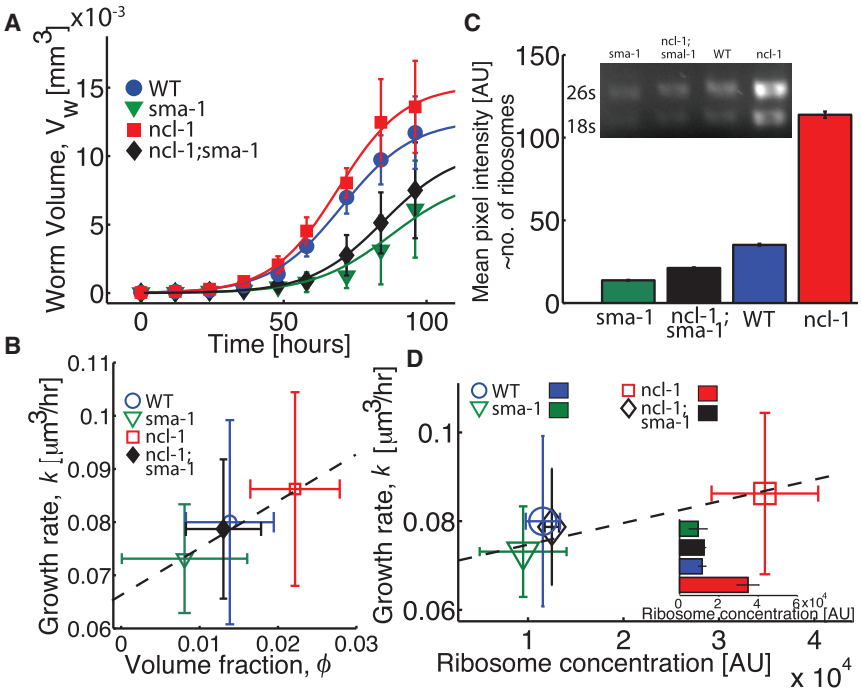

Figure 4. Functional Consequences of Nucleolar Size

(A) Volumetric growth curves for worms. Data are symbols, and lines are logistic growth fits. R^2 values for goodness of logistic growth fit are as follows: $R^2_{WT} = 0.99$, $R^2_{ncl} = 0.99$, and $R^2_{sma} = 0.96$, $R^2_{ncl;sma} = 0.99$, n = 9–10 worms per curve.

(B) Growth rate as function of volume fraction of cell occupied by nucleolus. Error bars indicate 95% confidence intervals to fit coefficients.

(C) Relative ribosomal content per genotype quantified as pixel intensity of 26-s rRNA band in gel shown in inset. Error bars indicate SEM. Inset: rRNA extracted from 50 L4 worms of each genotype run on 1% agarose ethidium bromide gel.

(D) Increased apparent ribosomal concentration correlates with faster growth rates. Error bars on the x axis indicate SEM, and error bars on the y axis indicate 95% confidence intervals to fit coefficients. Inset: apparent ribosome concentration by genotype calculated using ribosome number (represented by intensity values in C) normalized by L4 worm volume (from A).

and could be elucidated with further study of different cell types.

Despite 2-fold differences in the size of cells within the intestine, for both the nucleus and the nucleolus, the scaling in all cell data can be superimposed, suggesting that subcellular scaling is coordinated by a similar mechanism within each cell. This would manifest in coordinated growth across tissue-level length scales during multicellular growth. However, we note that the coordination of tissue-level growth and development is also thought to be achieved by regulated developmental milestones. Interestingly, mounting evidence suggests that several organisms, including *C. elegans,* cross these developmental milestones only when a critical organismal size has been achieved (Uppaluri and Brangwynne, 2015; Callier and Nijhout, 2011; Mirth et al., 2005); under slow-growth conditions, development is delayed until this critical size is reached. Thus, biophysically coupled scaling at the individual cell level, which manifests in coordinated tissue-level growth to a size threshold, could help coordinate development across diverse biological length scales.

Physiological processes require a constant exchange of material; molecular-level interactions are, therefore, intrinsically linked to the size of their compartment. Indeed, size is arguably one of the most important features of an organism, influencing both structure and function. The results presented here suggest that the size of subcellular structures has important consequences for larger length scale growth and should aid in the development of quantitative multiscale models of size control. This work thus points to the next frontier in organelle size scaling studies—to elucidate the mechanisms underlying scaling relationships across multiple levels of biological organization and to dissect their functional significance.

EXPERIMENTAL PROCEDURES

Worm Strains and Culture

Worms were maintained using standard methods at 20°C. To visualize nucleoli and nuclei in the intestine, *fib-1* was integrated into the pCPB007 plasmid containing the intestinal *vha-6* intestinal promoter and *mCherry* using gateway cloning. This construct was integrated into the worm genome by microparticle bombardment. All crosses were verified by PCR amplification of the mutation site followed by sequencing. See Table S2 for details regarding worm strains.

Microscopy

3D confocal images were obtained using an inverted Zeiss Axio Observer Z1 microscope equipped with a Yokogawa CSU-X1 confocal spinning disk (Intelligent Imaging Innovations) and a QuantEM 512SC camera (Photometrics) using a 40×/NA 1.4 oil immersion objective. Worm volumetric growth curves and intestinal volumes were obtained using a Leica M205FA fluorescence stereomicroscope (Wetzlar). For each genetic background, sample size, n, is reported as distinct biological replicates, as distinct worms were measured in parallel.

Image and Data Analysis

Images were passed through a 3D band-pass filter and thresholded with custom software in MATLAB, as reported by Weber and Brangwynne (2015). Thresholds were determined empirically for nucleoli and nuclei. Identical threshold values were used for all genetic backgrounds and developmental stages. Fitting and analysis were also conducted in MATLAB. Where applicable, fits were made to binned data.

The intestine and worm were approximated to a cylinder with ($V_{intest} = L\pi r^2$); the radius, r, and length, L, were measured manually using ImageJ. To obtain cell volumes, for each intestinal ring (int1 or int2), the length and radius were measured. These were used to obtain the volume of the cylinder occupied by the ring and then divided by the number of cells occupying that ring. The int1 ring comprises four cells, and the int2 ring comprises two cells. The intestine and intestinal cell membranes were visualized using the pvha6::PH::gfp background (see Table S2 for strain details).

Fluorescence Recovery After Photobleaching

FRAP experiments were conducted on a Nikon A1 inverted laser scanning confocal microscope, using a 40×/NA 1.3 oil immersion objective. Recovery of a bleached spot of a radius, r, of 1 μm inside the nucleolus was recorded. Intensity traces were corrected for photo-bleaching, normalized, and fit to an exponential function of the form $f(t) = A\left(1 - e^{-t/\tau}\right)$.

Ribosomal Extraction and Quantification

Total rRNA was extracted from the same number of L4 worms using TRIzol (Burdine and Stern, 1996) for each genotype and suspended in the same volume of TE buffer. Equal volumes of total RNA were electrophoresed on a 1% agarose gel stained with ethidium bromide. Ribosomes were quantified by subtracting mean background pixel intensity from mean pixel intensity in a given 26S band. Ribosomal concentration was obtained by dividing the mean pixel intensity in a given 26S band by the mean volume of the worm at the L4 stage extracted from logistic fit in Figure 4A. Error was propagated as SE.

SUPPLEMENTAL INFORMATION

Supplemental Information includes four figures and two tables and can be found with this article online at http://dx.doi.org/10.1016/j.celrep.2016.09.007.

AUTHOR CONTRIBUTIONS

S.U. and S.C.W. conducted the experiments. S.U. conducted data analysis. S.U., S.C.W., and C.P.B. designed the study and wrote the paper.

ACKNOWLEDGMENTS

We would like to thank Nilesh Vaidya, Shana Elbaum-Garfinkle, Carlos Chen, and the members of the C.P.B. lab for helpful discussions. Some strains were provided by the CGC, which is funded by the NIH Office of Research Infrastructure Programs (P40 OD010440).

This work was supported by the NIH Director's New Innovator Award (1DP2GM105437-01) and the Searle Scholars Program (12-SSP-217). S.C.W. was funded by the Damon Runyon Cancer Research Foundation.

Received: April 29, 2016
Revised: July 12, 2016
Accepted: September 1, 2016
Published: October 4, 2016

REFERENCES

Berry, J., Weber, S.C., Vaidya, N., Haataja, M., and Brangwynne, C.P. (2015). RNA transcription modulates phase transition-driven nuclear body assembly. Proc. Natl. Acad. Sci. USA *112*, E5237–E5245.

Brangwynne, C.P. (2013). Phase transitions and size scaling of membrane-less organelles. J. Cell Biol. *203*, 875–881.

Brangwynne, C.P., Eckmann, C.R., Courson, D.S., Rybarska, A., Hoege, C., Gharakhani, J., Jülicher, F., and Hyman, A.A. (2009). Germline P granules are liquid droplets that localize by controlled dissolution/condensation. Science *324*, 1729–1732.

Brangwynne, C.P., Mitchison, T.J., and Hyman, A.A. (2011). Active liquid-like behavior of nucleoli determines their size and shape in Xenopus laevis oocytes. Proc. Natl. Acad. Sci. USA *108*, 4334–4339.

Burdine, R.D., and Stern, M.J. (1996). Easy RNA isolation from C. elegans: a TRIZOL based method. Worm Breed. Gaz. *14*, 10.

Callier, V., and Nijhout, H.F. (2011). Control of body size by oxygen supply reveals size-dependent and size-independent mechanisms of molting and metamorphosis. Proc. Natl. Acad. Sci. USA *108*, 14664–14669.

Decker, M., Jaensch, S., Pozniakovsky, A., Zinke, A., O'Connell, K.F., Zachariae, W., Myers, E., and Hyman, A.A. (2011). Limiting amounts of centrosome material set centrosome size in C. elegans embryos. Curr. Biol. *21*, 1259–1267.

Derenzini, M., Montanaro, L., and Treré, D. (2009). What the nucleolus says to a tumour pathologist. Histopathology *54*, 753–762.

Edens, L.J., White, K.H., Jevtic, P., Li, X., and Levy, D.L. (2013). Nuclear size regulation: from single cells to development and disease. Trends Cell Biol. *23*, 151–159.

Fankhauser, G. (1939). Polyploidy in the salamander, Eurycea bislineata. J. Hered.

Fankhauser, G., and Humphrey, R.R. (1943). The relation between number of nucleoli and number of chromosome sets in animal cells. Proc. Natl. Acad. Sci. USA *29*, 344–350.

Feric, M., and Brangwynne, C.P. (2013). A nuclear F-actin scaffold stabilizes ribonucleoprotein droplets against gravity in large cells. Nat. Cell Biol. *15*, 1253–1259.

Frank, D.J., and Roth, M.B. (1998). ncl-1 is required for the regulation of cell size and ribosomal RNA synthesis in Caenorhabditis elegans. J. Cell Biol. *140*, 1321–1329.

Frank, D.J., Edgar, B.A., and Roth, M.B. (2002). The Drosophila melanogaster gene brain tumor negatively regulates cell growth and ribosomal RNA synthesis. Development *129*, 399–407.

Good, M.C., Vahey, M.D., Skandarajah, A., Fletcher, D.A., and Heald, R. (2013). Cytoplasmic volume modulates spindle size during embryogenesis. Science *342*, 856–860.

Hazel, J., Krutkramelis, K., Mooney, P., Tomschik, M., Gerow, K., Oakey, J., and Gatlin, J.C. (2013). Changes in cytoplasmic volume are sufficient to drive spindle scaling. Science *342*, 853–856.

Hertwig, R. (1903). Ueber die Korrelation von Zell-und Kerngrösse und ihre Bedeutung für die Geschlechtliche Differenzierung und die Teilung der Zelle. [On the correlation of cell and nuclear size and its significance for the sex distinction and the division of the cell.]. Biologisches Centralblatt *23*, 49–62.

Huxley, J.S. (1924). Constant differential growth-ratios and their significance. Nature *114*, 895–896.

Huxley, J.S., and Teissier, G. (1936). Terminology of relative growth. Nature *137*, 780–781.

Jorgensen, P., Edgington, N.P., Schneider, B.L., Rupes, I., Tyers, M., and Futcher, B. (2007). The size of the nucleus increases as yeast cells grow. Mol. Biol. Cell *18*, 3523–3532.

Lapicque, L. (1907). Tableau général des poids somatiques et encéphaliques dans les espèces animales. [General picture of body and brain weight in animal species.]. Bulletins et Memoires de la Societe d Anthropologie de Paris *8*, 248–270.

Lozano, E., Sáez, A.G., Flemming, A.J., Cunha, A., and Leroi, A.M. (2006). Regulation of growth by ploidy in Caenorhabditis elegans. Curr. Biol. *16*, 493–498.

McGhee, J.D. (2007). The C. elegans intestine. WormBook, 1–31.

McKeown, C., Praitis, V., and Austin, J. (1998). sma-1 encodes a betaH-spectrin homolog required for Caenorhabditis elegans morphogenesis. Development *125*, 2087–2098.

Mirth, C., Truman, J.W., and Riddiford, L.M. (2005). The role of the prothoracic gland in determining critical weight for metamorphosis in Drosophila melanogaster. Curr. Biol. *15*, 1796–1807.

Molliex, A., Temirov, J., Lee, J., Coughlin, M., Kanagaraj, A.P., Kim, H.J., Mittag, T., and Taylor, J.P. (2015). Phase separation by low complexity domains promotes stress granule assembly and drives pathological fibrillization. Cell *163*, 123–133.

Montagne, J., Stewart, M.J., Stocker, H., Hafen, E., Kozma, S.C., and Thomas, G. (1999). Drosophila S6 kinase: a regulator of cell size. Science *285*, 2126–2129.

Neumann, F.R., and Nurse, P. (2007). Nuclear size control in fission yeast. J. Cell Biol. *179*, 593–600.

Rafelski, S.M., Viana, M.P., Zhang, Y., Chan, Y.-H.M., Thorn, K.S., Yam, P., Fung, J.C., Li, H., Costa, Lda.F., and Marshall, W.F. (2012). Mitochondrial network size scaling in budding yeast. Science *338*, 822–824.

Rudra, D., and Warner, J. (2004). What better measure than ribosome synthesis? Genes Dev. *18*, 2431–2436.

Scott, M., Gunderson, C.W., Mateescu, E.M., Zhang, Z., and Hwa, T. (2010). Interdependence of cell growth and gene expression: origins and consequences. Science *330*, 1099–1102.

Tsang, C.K., Bertram, P.G., Ai, W., Drenan, R., and Zheng, X.F.S. (2003). Chromatin-mediated regulation of nucleolar structure and RNA Pol I localization by TOR. EMBO J. *22*, 6045–6056.

Uppaluri, S., and Brangwynne, C.P. (2015). A size threshold governs Caenorhabditis elegans developmental progression. Proc. Biol. Sci. *282*, 20151283.

Weber, S.C., and Brangwynne, C.P. (2015). Inverse size scaling of the nucleolus by a concentration-dependent phase transition. Curr. Biol. *25*, 641–646.

Wilson, E.B. (1896). The Cell in Development and Inheritance (New York: The Macmillan Company).

Wühr, M., Chen, Y., Dumont, S., Groen, A.C., Needleman, D.J., Salic, A., and Mitchison, T.J. (2008). Evidence for an upper limit to mitotic spindle length. Curr. Biol. *18*, 1256–1261.

Yang, X., and Xu, T. (2011). Molecular mechanism of size control in development and human diseases. Cell Res. *21*, 715–729.